SWIRL INJECTOR NOZZLE PROFILE FOR DIFFERENT SPATICIAL MASS DISTRIBUTIONS AND SPRAY DISPERSIONS

E. Abo-Serie, F. Abdl-Aziz, M. Afify, and H. Kayed

Department of Mechanical Power Engineering, Cairo University, Egypt

Abstract

Injecting liquid spray using a surface mounted swirl injector in a gas pipe flow to achieve a uniform mixture within a limited distance from the injector location is a challenging problem. The spatial distribution of liquid mass has to be directly related to the mass of gas distribution in the pipe. It is therefore necessary to be able to control the liquid mass spatial distribution within the gas pipe to have similar liquid to gas ratio throughout the pipe. This work analyzes the mass distribution from a swirl injector that has any nozzle cut profile. An equation has been derived to estimate the nozzle circumferential distribution of the mass relative to the total mass exiting the nozzle. The equation requires the nozzle flow angle and profile of the nozzle cut. The flow angle at the nozzle exit has been estimated using a CFD single phase calculations. The final results provide a guideline for the designer to the required nozzle cut profile to achieve a specific circumferential mass distribution. The expected spray shape based on the mass distribution exiting the nozzle has been similar to what has been shown from the spray images. Further work will be carried out to optimize the nozzle cut for different gas flow profiles.

Introduction

Swirl injector is used in many applications due to its better atomization and wide dispersion with lower energy relative to other commonly used pressure injectors. The swirl motion created by the swirler inside the injector leads to a centrifugal force that pushes the injected liquid to form a film attached to the nozzle-hole wall and leaving a central air core of low pressure [1] in the hole. As the liquid film exits the nozzle, it provides uniform mass distribution and forms a hollow cone spray for a flat face cut nozzle. The analysis of the liquid film thickness and the profile for a flat face cut nozzle has been previously studied [2]. One of the major problems of the swirl injector with a flat face nozzle is the change of its spray geometry with the surrounding conditions and the nozzle tip temperature [3]. Previous study [4] showed that having the nozzle cut with a fixed angle smaller than the liquid flow angle measured from the nozzle centreline leads to an open hollow cone spray without deterioration in the atomization quality. The study showed also that the cut angle can control the mass distribution from across the circumference of the nozzle. Therefore, to form an open side spray a previous knowledge about the flow angle.

Flow angle α is the angle between the flow velocity vector at the nozzle exit and the nozzle axis. The angle is mainly controlled by the swirler design and the nozzle length. The flow angle can be assumed equal to half the spray angle [1,5]. In another study [6], it was found that the predicted flow angle is usually higher than the spray angle and suggested a correction factor of 0.6315. The analysis for the flow near to the nozzle exit revealed that the spray opening angle increases until it reaches an asymptotic value which is equal to the spray angle [3]. The final spray angle, therefore, depends on both film and droplet penetrations outside the nozzle. The analysis showed that factors such as nozzle film thickness, Weber number, pressure difference across the liquid film and the break-up length are all affecting the spray angle [2]. Different experimental techniques have been used to identify the flow angle; the simplest method is the use of direct imaging with longer exposure time [3]. Another method uses flourescence PIV technique [7]. The flow angle can also be estimated numerically provided that the nozzle geometry is known. Single phase and two phase simulations have been carried out [8].

Although most of the previous mentioned studies have been performed on a gasoline direct injection injectors, a continuous flow swirl injector can be found in many applications: agriculture, aircraft, painting, humidifiers [5]. Some of these applications require fixing the injector on the wall of the pipe to deliver a spray of liquid to the flowing gas and achieve a good mixing within a short distance from the injector. One example is the injection of Urea in the exhaust pipe of a diesel engine to reduce NOx [9]. Due to the close installation of the catalyst to the engine the Urea has to be injected and mixed before entering the catalyst with a uniform Urea to gas ratio within the available short distance. The use of mixer causes increase in engine back pressure leading to power loss while having central injector is not ideal due to the different technical problems and the partial blockage of gas flow. Mounting swirl injector with a fat face nozzle on the surface of the pipe leads to impingement and non uniform mixing.

In this study, the relationship between the nozzle cut profile and the mass distribution at the nozzle exit has been derived. To validate the results, a swirl injector has been manufactured and spray images has been obtained. An attempt to measure the mass flux has been made using a mechanical patternator.

Mass Flux Distribution Analysis

The objective here is to develop a methodology to estimate the mass distribution from any nozzle cut profile. The analysis assumes a uniform velocity at the nozzle exit in magnitude and direction. Moreover the film thickness at the nozzle exits is considered constant along the nozzle cut. Based on these assumptions a mathematical analysis has been adopted to estimate the volume rate fraction across the nozzle and the resultant spray shape for any cut angle. When the nozzle has simple cut of angle γ as shown in Figure 1, the relation between the height y at any point on the cut and its radial distance x can be expressed as:

$$y = f(x) = x \tan \gamma \qquad (1)$$

To understand the following analysis, the nozzle with a cut angle γ is unrolled and laid to be flat sheet as shown in Figure 2.

$$x = r\,(1-\cos\theta) \qquad (2)$$

$$y(\theta) = r \tan(\gamma)\,(1-\cos\theta) \qquad (3)$$

By assuming the thickness of the sheet, h, the flow angle, (90 - α), and the axial and tangential velocities are invariable along the circumference. The slope of the surface (ϕ) at certain angle (θ) can be found as:

$$\tan(\phi) = \frac{1}{r}\frac{dy}{d\theta} = \tan(\gamma)\sin(\theta) \qquad (4)$$

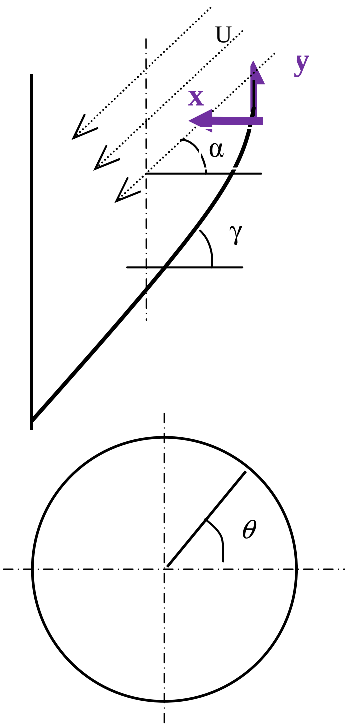

Figure 1: tapper nozzle of a cut angle γ and a flow angle α

To identify the exit volume flow rate from the taper nozzle, the velocity perpendicular to the nozzle exit plane has to be calculated for different angles of γ. From the geometry, the velocity normal to the nozzle exit plane is,

$$U_f = U \sin(\alpha - \phi) \qquad (5)$$

Where, U is the absolute flow velocity and α is the flow angle

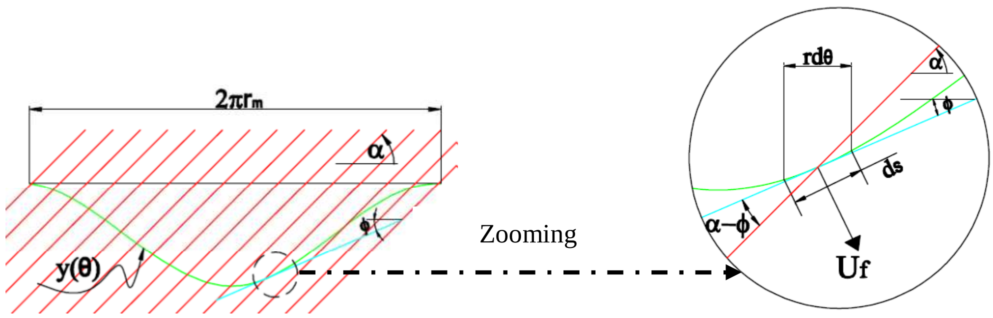

Figure 2: the unrolled tapper nozzle with a zooming on a point along its profile. The red colour displays the flow direction and the green colours depicts nozzle edge profile after unrolling and its tangent.

The exit volume flow rate at any dθ can be evaluated from

$$dV = U_f \ ds \qquad (6)$$

The outlet area through an angle dθ

$$ds = \frac{rd\theta}{cos\Phi} h \qquad (7)$$

Combining equations (5) and (7) to evaluate the exit volume flow rate through an angle dθ

$$dV = u_f * ds = \mathrm{U} * \sin(\alpha - \Phi) * \frac{rd\theta}{cos\Phi} h \qquad (8)$$

From trigonometry, $\sin(\alpha - \Phi) = \sin\alpha\cos\Phi - \cos\alpha\sin\Phi$, substituting equation (5) and rearranging

$$dV = rhud\theta[\sin(\alpha) - \cos(\alpha)\tan(\gamma)\sin(\theta)] \qquad (9)$$

The total inlet volume flow rate to the nozzle is $V_t = 2\pi \mathrm{r_m hU}\sin(\alpha)$. Therefore, mass fraction out from tapered nozzle with cut angle (γ) is

$$\frac{dm}{m_t} = [1 - \frac{tan(\gamma)}{tan(\alpha)} * sin(\theta)] * \frac{d\theta}{2\pi} \qquad (10)$$

It can be concluded that the fractional mass is functional of the flow angle α, the nozzle cut angle γ and the arc angle (dθ). Therefore it can be estimated at each arc angle (dθ) over the full circumference of the nozzle (2π).

Clearly as the cut angle increases, the quantity of liquid fuel exiting from one side decreases until it reaches a critical value where no mass exiting the nozzle, at a specific location which is correspond to ($\phi = \alpha$). At this critical cut angle, the liquid inside the nozzle moves parallel to the nozzle cut edge without exiting the nozzle.
If ($\phi > \alpha$) the spray side starts to open and no fuel exits between θ_1 and θ_2 as shown in Figure 3.

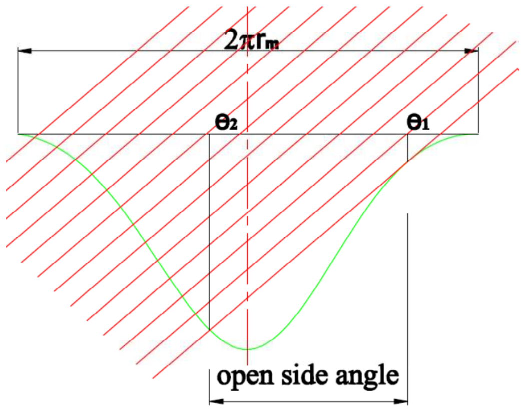

Figure 3: open side angle between θ_1 and θ_2

At $\phi = \alpha$, $\tan\phi = \tan\alpha$, and from equation *(4);*

$$sin\ \theta_1 = \frac{tan(\alpha)}{tan(\gamma)} \qquad (11)$$

The equation of straight line in figure 3 shows that

$$\frac{y_2 - y_1}{r(\theta_2 - \theta_1)} = tan(\alpha) \qquad (12)$$

$$y_2 - y_1 = r(\theta_2 - \theta_1) * tan(\alpha) \qquad (13)$$

$$r\tan(\gamma)\,(1 - cos\theta_2) - r\tan(\gamma)\,(1 - cos\theta_1) = r(\theta_2 - \theta_1) * tan(\alpha) \qquad (14)$$

$$\theta_1 - \theta_2 + \frac{\tan\gamma}{\tan\alpha}(\cos\theta_1 - \cos\theta_2) = 0 \qquad (15)$$

The actual angle could be larger than the value calculated here, due to the thickening of the edge of the liquid film after exiting the nozzle and before being atomized, as observed in other studies using fan sprays [11].

Equation *(10)* can be generalized to have the distribution of spray volume fraction for any cut profile $y = f(x)$.

$$\frac{dm}{m_t} = [1 - \frac{\bar{y}'}{\tan(\alpha)} * \sin(\theta)] * \frac{d\theta}{2\pi} \qquad (16)$$

Where $\bar{y}' = \frac{d\bar{y}}{d\bar{x}}\Big|_{x=0.5(1-\cos\theta)}$ $\quad \bar{y} = y/D, \quad \bar{x} = x/D$

For the notch profile case equation (16) becomes;

$$\frac{dm}{m_t} = [1 - \frac{\bar{y}'}{\tan(\alpha)} * \sin(\theta + k)] * \frac{d\theta}{2\pi} \qquad (17)$$

Where $k = \pi$ for $\theta = (\pi/2$ to $3\pi/2)$, otherwise $k = 0$;

The generic location where the spray starts to open from θ_1 to θ_2 takes place when ($\Phi \geq \alpha$). At which θ_1 ,θ_2 can be evaluated as follows;

$$\sin\theta_1 = \frac{\bar{y}'}{\tan(\alpha)} \qquad (18)$$

$$\theta_1 - \theta_2 + \frac{\bar{y}'}{\tan\alpha}(\cos\theta_1 - \cos(\theta_2 + \mathrm{k})) = 0 \qquad (19)$$

Injector Design and Flow Simulation

In order to validate the mathematical analysis, a swirl injector has been manufactured from an Acrylic material as shown in Figure 4 and a continuous water flow has been admitted with different injection pressures. The injector has four tangential holes located inside the casing that generates the swirling motion as shown in Figure 5. The flow exits the holes into a hollow conical passage before exiting the hole as shown in the mesh simulation. The hole has been cut with a fixed cut angle γ of 70 degree to have a face that is inclined by 20 degree on the axis of the hole. An attempt has been made to design and manufacture a patternator made of 8 tubes separated with specific known distances shown in Figure 6.

The flow inside the injector has been simulated using STARCCM+. Isothermal incompressible steady turbulent flow, single phase has been considered to simulate the flow inside the nozzle. The RNG k-ε model was used owing to its simplicity and robustness [11]. Non uniform mesh has been employed with much smaller cells near the wall. The aim of the simulation is to estimate the flow angle at the nozzle exit.

	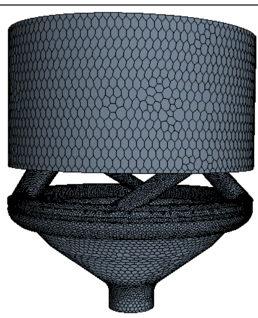	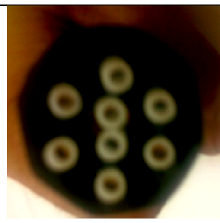
Figure 4 Swirl injector nozzle with a 60 degree cut angle	Figure 5 Mesh of the fluid flow inside the swirling nozzle	Figure 6 Frontal picture of the mechanical patternator

Results and Discussion

In the following sections the results of experimental work and simulations for a fixed cut angle followed by a the results of the mass distribution for three different nozzle cut profiles will be shown.

Spray images and flow angle estimation

The experimental work was applied on the nozzle that has been manufactured for validation purpose. Although this case has been examined previously on a gasoline direct injection injector [4], it has been repeated here using a continuous flow of water with low injection pressure to validate the general equation that has been derived above. The typical tulip shape of the spray at low injection pressure can still be seen with a nozzle cut 70 degree as shown in figure 7. This is attributed to the small value of the tangential velocity relative to the axial velocity at low injection pressure. Further increase in the injection pressure leads to the developed shape of the spray as shown in Figure 8. By rotating the camera it was clearly shown that the spray are produced from one side of the nozzle and no flow exits from the other side as shown in Figure 9. The spray angle was estimated to be 60 degree for this injector.

		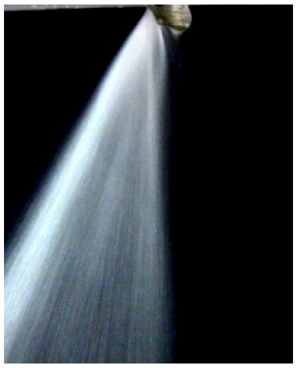
Figure 6 typical tulip shape of the spray at low injection pressure	Figure 7 Frontal view of the fully developed spray	Figure 8 Side view of the fully developed spray

If the flow angle is assumed equal to half the spray angle [1,5] then according to the spray images shown in Figure 7, its value is approximately 30 degree. The CFD simulation showed much higher flow angle. The value of the flow angle changed depending on the method used to calculate it. A mass average angle at the nozzle exit showed a value of 49 degree while a value of 47 degree was found when the maximum axial and tangential velocities are used to calculate the flow angle. If the values of the flow angle are multiplied by the 0.6315 which is proposed in a previous study [6] to calculate half the spray angle, the result will be 29.6 - 30.9 degree. This value was in agreement with the measured spray angle. The maximum value may be considered more representing than the average value as previous researchers showed that the single phase simulation underestimates the flow angle in comparison to the experiments and the Volume Of Fluid VOF two phase computational method [11]. The streamlines for the flow inside the nozzle showing the rotation of flow inside the nozzle is shown in Figure 9.

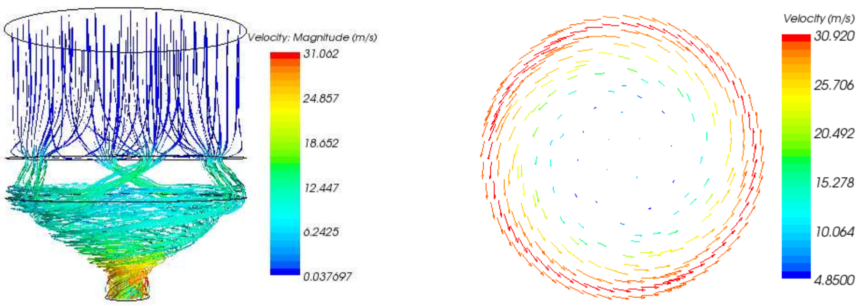

Figure 9 Streamlines of internal nozzle flow and velocity vectors at the nozzle exit

Mass flux distributions for fixed angle nozzle cut

The mass flux from three nozzle cuts 30, 50 and 70 degree have been examined under a fixed flow angle of 30 degree measured from the nozzle axis, see Figure 10. The mass distributions for the three nozzle cuts are shown in Figure 11. The figure shows the uneven mass flux distribution across the nozzle circumference. Moreover, the liquid film inside the nozzle hollow cone spray starts to open up at one side of the nozzle when the complement of the flow angle becomes equal to cut angle ($\alpha = \gamma = 30°$). As the cut angle γ becomes larger, the flow in one side of the nozzle cannot exit and moves inside the wall until it reaches the other side of the nozzle. An open side spray with a more fan spray than a conical spray structure is formed with the increase in the nozzle cut angle. These results have been previously verified in a GDI swirl injector and also shown in the images of the sprays taken from the current manufactured injector, shown previously in Figure 8. Since the mass flow distribution is the result of the normal velocity times the area times the density, it is of interest to examine the change in the normal velocity and area with the angle θ. Although the area are symmetric as shown in Figure 12 the normal velocity in the upper side of the graph is very small as shown in Figure 13. Therefore the mass exiting from the bottom part is much more than the upper part of the nozzle. For the 70 degree cut angle part of the nozzle does not allow any mass to exit and therefore an arc spray shape is formed.

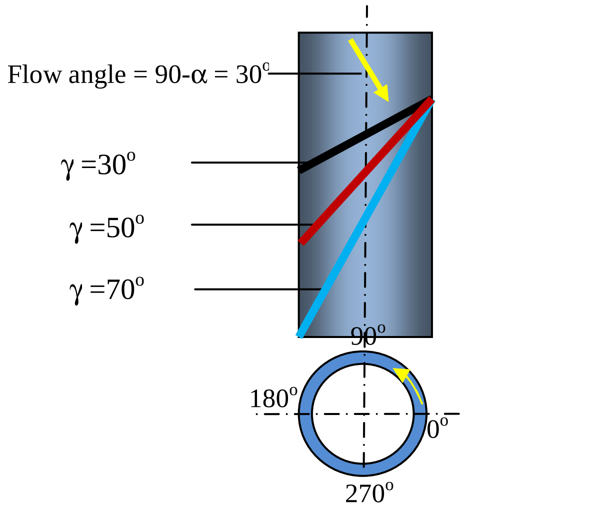

Figure 10 Schematic showing the three fixed angle nozzle cuts

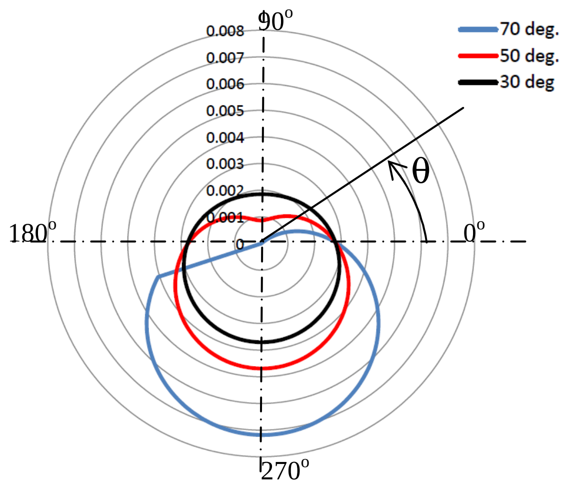

Figure 11 The circumferential mass distribution for the three nozzle cuts

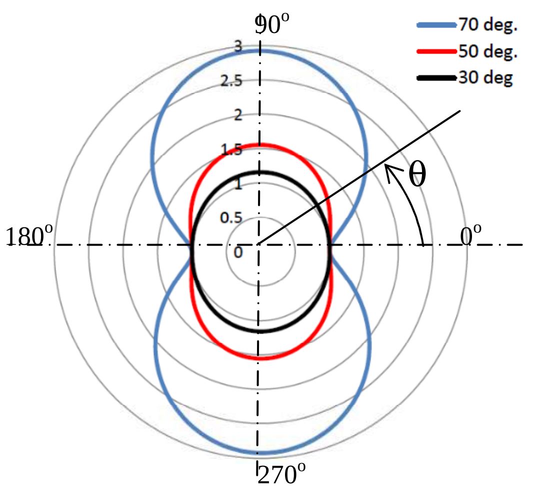

Figure 12 the relative arc area relative to the arc area for a flat nozzle

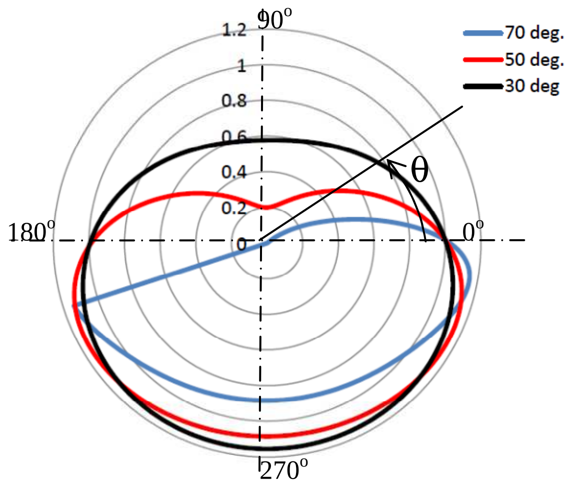

Figure 13 the normal velocity distribution relative to the aveage axial velocity at the nozzle exit

Mass flux distributions for a notch nozzle cut

Similar analysis has been performed for three notch nozzle of different angles 30, 50 and 70 degree as shown in Figure 14. Figure 15 shows the mass flux distribution relative to the total mass. Each graph shows two similar mass distribution and both the 30 and 50 notch cut angle have liquid flow from all the circumference of the nozzle but with different mass. However the case of 70 degree notch angle will produce two symmetric wings of spray. The length of the arc producing the wing spray decreases as the angle increases. Figure 16 shows the area corresponds to one degree angle along the circumference of the nozzle. The figure also shows symmetric shape with respect to the horizontal axis. The normal velocity shows two similar profiles on each side of the nozzle as shown in Figure 17. Attempts have been made to validate the mass distribution using the mechanical patternator shown in Figure 6 but the reflection of water droplets causes ambiguous and non repeatable results. It was therefore decided not to include the results here and to use optical techniques in a later stage.

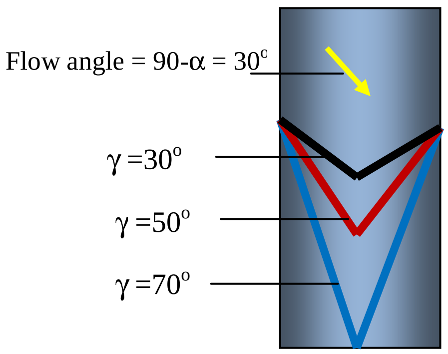

Figure 14 Schematic showing the three notch nozzle cuts

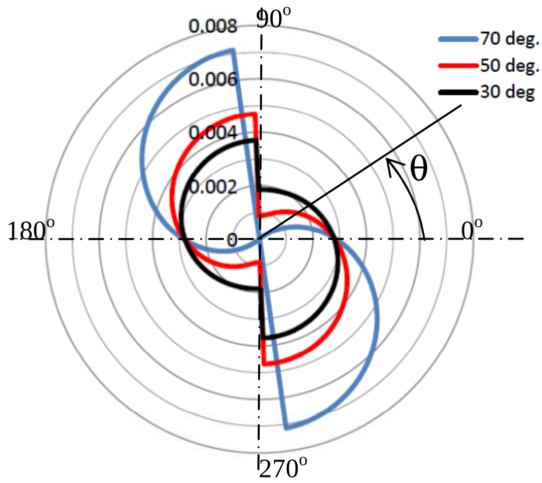

Figure 15 The circumferential mass distribution for the three nozzle cuts

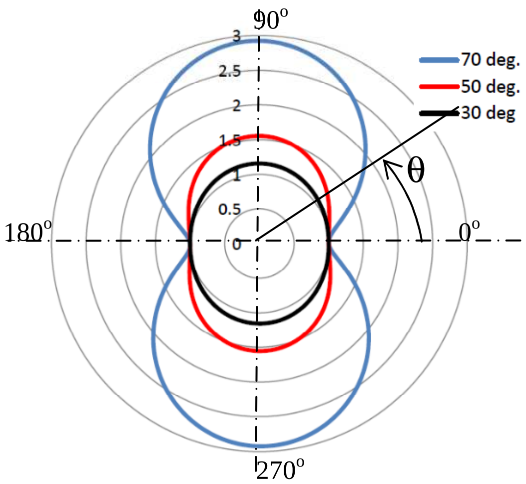

Figure 16 the relative arc area relative to the arc area for a flat nozzle

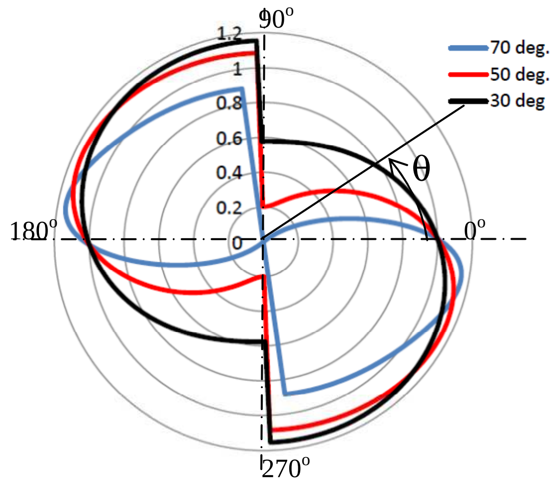

Figure 13 the normal velocity distribution relative to the aveage axial velocity at the nozzle exit

Conclusions:

A mathematical analysis has been performed to calculate the mass distribution along the circumference of a swirl nozzle that can be cut with specific profile; y = f(x). The analysis therefore is valid for a symmetric nozzle cut. The results shows different spray shapes can be produced with non uniform mass flux. Two case studies has been considered, the first for a fixed angle cut and the second for a notch nozzle cut. The expected shape of the spray for the first case has been obtained using direct images for the first case nozzle using a manufactured swirl injector. Although the study provides the mass distribution and the expected spray structure for different nozzle cuts, however the designer has to choose the right cut profile for the relevant problem. The study showed that the swirl injector nozzle cuts can produce different spray with different mass distribution and therefore has a potential to produce a liquid spray that can match the gas mass distribution. Matching the liquid mass distribution to the mass of gas has many applications and it is always a challenging problem especially in combustion systems.

Nomenclature

D nozzle diameter [m]
h film thickness [m]
m mass flow rate [kg/s]
r nozzle radius [m]
s arc area [m^2]
U flow velocity [m/s]
V volume flow rate [m^3/s]
x the distance from the nozzle centre to any point on the circumferential profile of the nozzle cut [m]
y the height at any point on the circumferential profile of the nozzle cut [m]
α flow angle [radian]
ϕ slope angle of any point on the circumferential profile of the nozzle cut [radian]
γ cut angle [degree]
θ the revolution angle varies from 0 to 2π around the axis of the nozzle [radian]

Subscripts
f flow velocity normal to nozzle exit plane
m mean
t total

References

[1] Ren, W. M. and Nally Jr, J. F. *Society of Automotive Engineering SAE* 982610, (1998)
[2] Moon, S, Bae, C, and Abo-Serie, E. F., *Atomization and Sprays* 3: 235-246 (2009)
[3] VanDerWege, B. and Hochgreb, S., *Society of Automotive Engineering*, *SAE* 2000-01-0536, (2000)
[4] Moon, S.,Abo-Serie, E. F. and Bae, C., *International Journal of Multiphase Flow*, 7: 615-627 (2008)
[5] Lefebvre, A. H. *Atomization and Sprays*, Hemisphere publishing corporation, 1989
[6] Cousin, J. and Nuglisch, *European Conference on Liquid Atomization and Spray Systems*, Toulouse, France, July, 1999
[7] Khoo, Y. C. and Hargrave, G. K., *Journal of Physics: Conference Series* 45: 77–84, (2006)
[8] Kubo, M., Sakakida, A. and Iiyama, A., *Society of Automotive Engineering*, 2001-01-0964, (2001)
[9] Johansson, A., Wallin, U., Karlsson, M, Isaksson, A. And Bush, P., *Society of Automotive Engineering*, *SAE* 2008-01-0613, (2008)
[10] Dombrowski N, Hasson D, Wand E., Chem Eng Sci., 2:35–50, (1960)
[11] Ren, W. M., Shen, J. And Nalley Jr, J. F. *Society of Automotive Engineering SAE* 971641, (1997)